

Electronic Supplement: Imbalance Settlement and Multi-Product Balancing Energy Markets

Jacques Cartuyvels, Gilles Bertrand, Alexandros Visas,
Anthony Papavasiliou

July 2025

1 Balancing Capacity Markets

The sequence of markets updated to account for balancing capacity markets is presented in Fig. 1. The capacity auctions (also called *reserve auctions*) are assumed to be held consecutively¹. They generate balancing capacity prices, P_{cap}^{aFRR} and P_{cap}^{mFRR} , based on the aFRR and mFRR capacity demand curves and the balancing capacity bids of the fast and slow assets.

The fast assets that are not selected can compete in the mFRR capacity auction with the slow assets. The capacity that is cleared in either the aFRR or the mFRR capacity auction has to be offered to the corresponding energy auction. The capacity that is not cleared can either participate in one of the energy auctions through so-called free bids or self-dispatch.

Modeling balancing capacity markets requires the introduction of the gate closure forecast, w , drawn from the random variable W . It represents the information available at the gate closure of the balancing energy auctions and allows

¹The product of higher quality, aFRR, is assumed to be auctioned first in our analysis. The joint co-optimized procurement of aFRR and mFRR balancing capacity is out of scope, although this is a very active field of debate at present, for instance in the UK.

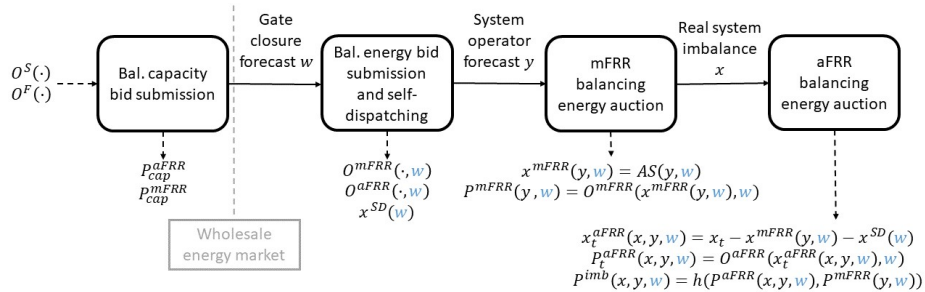


Figure 1: Sequence of markets and revelation of uncertainty with balancing capacity markets.

for multiple equilibria.² Each equilibrium as a function of w can be analyzed independently. The gate closure forecast was already introduced in the results section.

Balancing capacity markets interact with both the wholesale energy market and the balancing energy markets. The need for balancing capacity markets stems from an opportunity cost for participating in the balancing energy markets. If wholesale day-ahead or intraday energy markets are more profitable than balancing energy markets, flexible assets need additional incentives to participate in the balancing energy auctions. This analysis does not explicitly account for the wholesale market but it shows the potential opportunity cost that can be generated by combinations of mFRR activation strategies, imbalance pricing schemes, and capacity demand curves.

This analysis will describe the strategy sets for players participating in the game described in Fig. 1 and will then characterize equilibrium for the corner case with full capacity demand curves, and illustrate it on the example of subsection 1.3.

1.1 Strategy sets with Capacity Markets

The full game with balancing capacity markets is presented in Fig. 2. The strategy set for an agent with marginal cost θ participating in this game is the concatenation of the strategy set of the initial game for every possible realization of gate closure forecast (see Eqs. (10) and (13) of the main manuscript), $(q^{aFRR}(w), q^{mFRR}(w), q^{SC}(w))$, and the aFRR and mFRR capacity prices, p_{cap}^{aFRR} and p_{cap}^{mFRR} .³

$$\begin{aligned} \mathcal{Q}^F(\theta) = \{ & (p_{cap}^{aFRR}, p_{cap}^{mFRR}, q^{aFRR}, q^{mFRR}, q^{SD}) \mid \\ & q^{aFRR} + q^{mFRR} + q^{SD} = 1, \\ & q^{aFRR} \geq 0, q^{mFRR} \geq 0, q^{SD} \geq 0 \} \end{aligned} \quad (1)$$

The optimal strategy of this game is obtained through backward induction by starting at the bottom of the tree at the aFRR and mFRR activation payoffs and the self-dispatching payoff. The payoff of the non-reserved capacity is then back-propagated to the mFRR capacity auction and then to the aFRR capacity auction.

The energy activation stage, after w is revealed, is not impacted by the balancing capacity auctions and the payoff of the non-reserved capacity, z^{pow} , can be formulated as the expectation over the realization of w of the maximum

²Article 8.2 of the *Implementation Framework for the European Platform for the Exchange of Balancing Energy from Frequency Restoration Reserve with Automatic Activation*.

³In practice, agents must submit a price-quantity bid for the mFRR and aFRR balancing capacity auctions, $(p_{cap}^{aFRR}, q_{cap}^{aFRR})$ and $(p_{cap}^{mFRR}, q_{cap}^{mFRR})$. We only consider pure strategies between the aFRR and mFRR balancing capacity auctions, thus the quantity component of the balancing capacity bid is set at the maximum of the capacity.

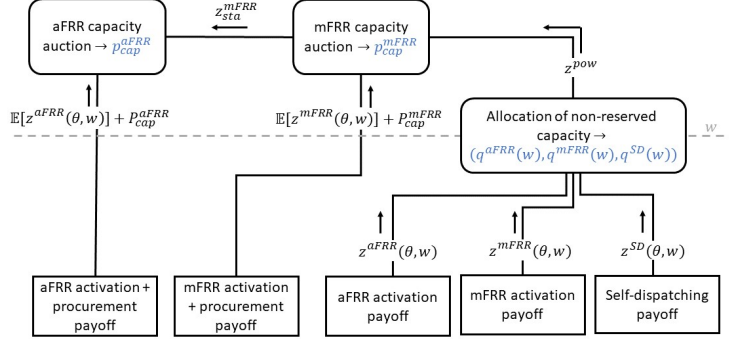


Figure 2: Strategy set and potential market opportunities with balancing capacity market.

of the aFRR and mFRR balancing energy payoff and the self-dispatching payoff. The non-reserved payoff, z^{pow} , can thus be expressed as follows:

$$z^{pow} = \int \max(z^{aFRR}(\theta, w); z^{mFRR}(\theta, w); z^{SD}(\theta, w)) dF_W(w) \quad (2)$$

The expected non-reserved payoff is then backpropagated to the mFRR capacity auction (see top-right of Fig. 2). The tradeoff between (i) participating in the mFRR balancing capacity auction and then in the mFRR balancing energy auction and (ii) participating in the balancing market as non-reserved capacity corresponds to the price component of the balancing capacity bid. It determines whether a bid is selected in the capacity auction and is sufficient for characterizing pure strategies. As in the case of non-reserved capacity, bidding the marginal cost in the subsequent balancing energy auction is weakly dominant. The optimal bidding strategy at this stage can then be found by solving Eq. (3) given an exogenous mFRR capacity price P_{cap}^{mFRR} :

$$\max_{p_{cap}^{mFRR}} \begin{cases} P_{cap}^{mFRR} + \mathbb{E}_W[z^{mFRR}(\theta, w)] & \text{if } p_{cap}^{mFRR} \leq P_{cap}^{mFRR} \\ z^{pow} & \text{if } p_{cap}^{mFRR} > P_{cap}^{mFRR} \end{cases} \quad (3)$$

Bidding the opportunity cost of participating in the mFRR balancing energy auction, $z^{pow} - \mathbb{E}_W[z^{mFRR}(\theta, w)]$, is always optimal. If $P_{cap}^{mFRR} + \mathbb{E}_{Y_1}[z^{mFRR}(\theta, w)] > z^{pow}$, then any price bid belonging to the interval $[0, P_{cap}^{mFRR}]$ is optimal. If $P_{cap}^{mFRR} + \mathbb{E}_{Y_1}[z^{mFRR}(\theta, w)] < z^{pow}$, then any price bid belonging to the interval $(P_{cap}^{mFRR}, +\infty)$ is optimal. This optimal strategy results in the expected payoff at the mFRR balancing capacity stage, z_{sta}^{mFRR} , being characterized as the maximum between the mFRR procurement and activation payoff and the payoff from not being reserved:

$$z_{sta}^{mFRR} = \max(P_{cap}^{mFRR} + \mathbb{E}_W[z^{mFRR}(\theta, w)]; z^{pow}) \quad (4)$$

The expected payoff at the mFRR capacity auction stage is then backpropagated to the aFRR capacity auction (see top-left of Fig. 2). The action space at that stage is similar to that of the mFRR capacity auction stage. The optimal bidding strategy is similar to the one in the mFRR capacity auction except that the tradeoff is between the aFRR procurement and activation payoff, $P_{cap}^{aFRR} + \mathbb{E}_W[z^{aFRR}(\theta, w)]$, and the expected payoff at the mFRR capacity auction stage. This results in the following price offer in the aFRR balancing capacity auction:

$$p_{cap}^{aFRR} = z_{sta}^{mFRR} - \mathbb{E}_W[z^{aFRR}(\theta, w)] \quad (5)$$

In summary, rational fringe agents participating in the multi-product reserve and energy balancing auction game (i) allocate their non-reserved capacity between the aFRR and mFRR balancing energy auction, as well as self-dispatching, depending on the highest activation payoff (bottom right of Fig. 2), (ii) bid the difference between solely participating in the mFRR balancing energy auction and participating in the balancing market as non-reserved capacity in the mFRR capacity auction (top right of Fig. 2), and (iii) bid the difference between solely participating in the aFRR balancing energy auction and the payoff at the mFRR capacity auction stage in the aFRR capacity auction (top left of Fig. 2).

1.2 Equilibrium with Full Capacity Demand Curve

The equilibria discussed in section IV of the main paper are corner cases of the complete multi-product reserve and energy games of Fig. 2 with zero aFRR and mFRR capacity demand curves. A second corner case of this game arises when the system operator uses *full capacity demand curves*, which procure the entirety of the balancing capacity for both fast and slow assets in the forward (day-ahead) market. This corresponds to inelastic reserve requirements for aFRR equal to the installed fast capacity and reserve requirements for mFRR equal to the installed slow capacity. This would correspond to aFRR and mFRR capacity demand curves of width N^F and N^S respectively. This scenario results in the following equilibrium.

Proposition 1. *The equilibrium with full capacity demand curves is characterized by every fast agent being selected in the aFRR capacity auction and every slow agent being selected in the mFRR capacity auction.*⁴

Proof. At equilibrium, the mFRR capacity price is equal to the difference in payoff between participating in the mFRR balancing energy auction versus participating in the balancing market as non-reserved capacity for the agent with the highest such cost, and the aFRR capacity price is equal to the maximum

⁴Technically, this equilibrium is generated from capacity demand curves that procure the entirety of the balancing capacity minus a small ϵ . The equilibrium requires a fringe agent to not be selected to ensure that the last agent that is selected in the balancing capacity auction bids its opportunity cost.

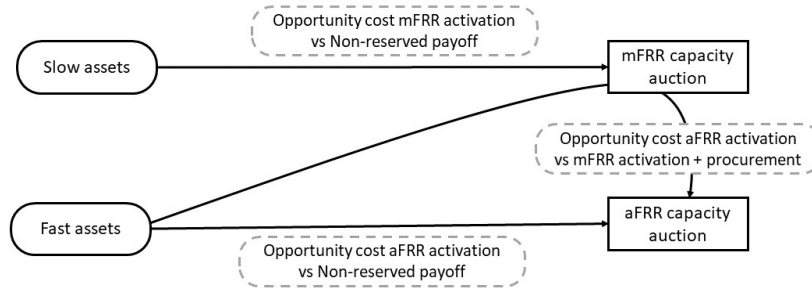


Figure 3: Opportunity cost in the capacity auctions.

between (a) the difference between participating in the aFRR balancing energy auction versus participating in the balancing market as non-reserved capacity for the agent with the highest such cost, and (b) the difference between participating in the aFRR balancing energy auction versus participating in the mFRR balancing energy and balancing capacity auctions for the agent with the highest such cost. These opportunity costs are presented in Fig. 3. No price-taking agent has an incentive to deviate from the equilibrium given these capacity prices. \square

Full capacity demand curves result in mFRR and aFRR capacity prices that are equal to zero for the “mFRR only” imbalance pricing policy. Participating in the mFRR balancing energy auction is the optimal strategy for slow assets, therefore slow assets have no opportunity cost for doing so, which results in a zero mFRR capacity price. If there is no mFRR procurement payoff, participating in the aFRR balancing energy auction remains the optimal strategy for fast assets. They too have no opportunity cost, which results in a zero aFRR capacity price. More generally, every balancing energy market design, i.e. the combination of an mFRR activation strategy and an imbalance pricing scheme, that incentivizes agents to participate in the best quality auction they can will result in zero aFRR and mFRR balancing capacity prices. This includes the “mean mFRR and aFRR” imbalance price under the least-cost mFRR activation strategy.

Balancing energy market designs that do not incentivize agents to offer their capacity in the best quality balancing energy auction can generate non-zero balancing capacity prices. Slow assets require a compensation for participating in the mFRR balancing energy auction if it is not their optimal strategy. Even if participating in the aFRR balancing energy auction is still the optimal strategy for the fast non-reserved capacity, the mFRR procurement payoff pushes the aFRR capacity price up as this generates an opportunity cost between solely offering aFRR balancing energy and participating in the mFRR balancing capacity auction (see Fig. 3).

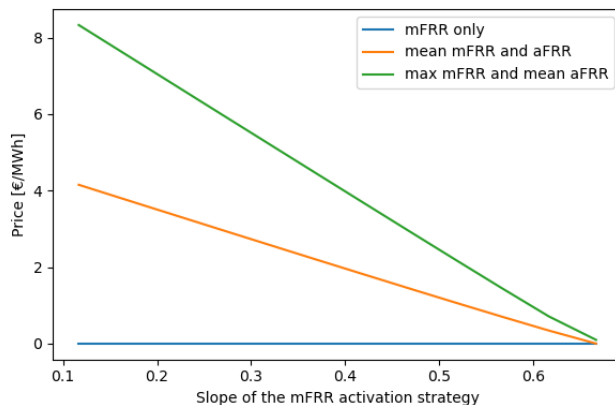


Figure 4: mFRR and aFRR capacity prices (which are equal) under full capacity demand curves for an mFRR activation strategy that is lower than or equal to that of the least-cost activation strategy for the example presented in section IV B of the main paper.

1.3 Capacity Prices with Full Capacity Demand Curves for the Illustrative Example

Self-dispatching can be restricted in the case of the “mean mFRR and aFRR” and the “max mFRR and mean aFRR” imbalance pricing schemes given sufficiently large capacity demand curves. The “mFRR only” imbalance price does not incentivize self-dispatching and generates zero capacity prices. This behavior and the resulting mFRR balancing capacity prices are presented in Fig. 4 for the illustrative example of the main paper. The horizontal axis in this figure represents the slope of a linear mFRR activation strategy up to the least-cost activation strategy at $2/3$. The lower the slope, the less mFRR is activated by the TSO, and the higher the opportunity cost of participating in the mFRR auction. Note that the aFRR balancing capacity prices are equal to the mFRR balancing capacity prices as the dominating opportunity cost in Fig. 3 is the one related to participating in the mFRR capacity auction.

2 Ramp Constraints and Upward and Downward Balancing Energy Markets

The least-cost activation strategy accounting for ramp constraints for aFRR is described hereunder given the inverse supply curves for upward and downward fast and slow capacity, $O^{F,u}(\cdot)$, $O^{F,d}(\cdot)$, $O^{S,u}(\cdot)$, and $O^{S,d}(\cdot)$, and the loss incurred with upward and downward loss, V^u and V^d . The disaggregation of the inverse supply curves for fast and slow assets into upward and downward inverse supply curves is necessary to account for the possible simultaneous activation

in both directions. Ramp constraints can force the system operator to activate a specific type of asset in both directions. Note that ramp constraints are only introduced for fast assets here. The introduction of ramp constraints for slow assets would require the analysis of multiple imbalance settlement periods.

In the model of Eqs (6a)-(6e), we present the least-cost activation problem accounting for ramp constraints. The fast and slow merit orders are disaggregated into upward, $O^{S,u}$ and $O^{F,u}$ respectively, and downward components, $O^{S,d}$ and $O^{F,d}$ respectively. The market clearing constraint for energy now includes upward and downward shortage variables, l^u and l^d , to prevent infeasible solutions arising from the ramp constraints on upward and downward fast reserve.

$$\min_{\substack{x^{S,u}, x^{S,d}, x_{t,\omega}^{F,u}, \\ x_{t,\omega}^{F,d}, l_{t,\omega}^u, l_{t,\omega}^d}} \int_0^{x^{S,u}} O^{S,u}(x)dx + \int_0^{x^{S,d}} O^{S,d}(x)dx + \mathbb{E}_\Omega \left[\sum_t \frac{1}{T} \left(\int_0^{x_{t,\omega}^{F,u}} O^{F,u}(x)dx \right. \right. \\ \left. \left. + \int_0^{x_{t,\omega}^{F,d}} O^{F,d}(x)dx + V^u \cdot l_{t,\omega}^u + V^d \cdot l_{t,\omega}^d \right) \right] \quad (6a)$$

$$s.t. \quad (\lambda_{t,\omega}) : \quad X_{t,\omega} = x^{S,u} - x^{S,d} + x_{t,\omega}^{F,u} - x_{t,\omega}^{F,d} + l_{t,\omega}^u - l_{t,\omega}^d \quad \forall t, \forall \omega \quad (6b)$$

$$(\mu_{t,\omega}^{u,-}, \mu_{t,\omega}^{u,+}) : \quad -R \leq x_{t,\omega}^{F,u} - x_{t+1,\omega}^{F,u} \leq R \quad \forall t, \forall \omega \quad (6c)$$

$$(\mu_{t,\omega}^{d,-}, \mu_{t,\omega}^{d,+}) : \quad -R \leq x_{t,\omega}^{F,d} - x_{t+1,\omega}^{F,d} \leq R \quad \forall t, \forall \omega \quad (6d)$$

$$x^{S,u}, x^{S,d}, x_{t,\omega}^{F,u}, x_{t,\omega}^{F,d}, l_{t,\omega}^u, l_{t,\omega}^d \geq 0 \quad (6e)$$

The first stage variables of the problem are the level of upward and downward slow reserve, $x^{S,u}$ and $x^{S,d}$. The recourse decisions are the level of downward and upward fast reserve activation in subperiod t and scenario ω , $x_{t,\omega}^{F,u}$ and $x_{t,\omega}^{F,d}$, and the upward and downward deviation from the balance in subperiod t and scenario ω , $l_{t,\omega}^u$ and $l_{t,\omega}^d$. The KKT conditions for the problem are described hereunder.

$$0 \leq x^{S,u} \perp O^{S,u}(x^{S,u}) - \mathbb{E}_\Omega \left[\sum_t \frac{1}{T} \lambda_{t,\omega} \right] \geq 0 \quad (7a)$$

$$0 \leq x^{S,d} \perp O^{S,d}(x^{S,d}) + \mathbb{E}_\Omega \left[\sum_t \frac{1}{T} \lambda_{t,\omega} \right] \geq 0 \quad (7b)$$

$$0 \leq x_{t,\omega}^{F,u} \perp O^{F,u}(x_{t,\omega}^{F,u}) - \lambda_{t,\omega} + \mu_{t,\omega}^{u,+} - \mu_{t,\omega}^{u,-} - \mu_{t-1,\omega}^{u,+} + \mu_{t-1,\omega}^{u,-} \geq 0 \quad (7c)$$

$$0 \leq x_{t,\omega}^{F,d} \perp O^{F,d}(x_{t,\omega}^{F,d}) + \lambda_{t,\omega} + \mu_{t,\omega}^{d,+} - \mu_{t,\omega}^{d,-} - \mu_{t-1,\omega}^{d,+} + \mu_{t-1,\omega}^{d,-} \geq 0 \quad (7d)$$

$$0 \leq l_{t,\omega}^u \perp V^u - \lambda_{t,\omega} \geq 0 \quad (7e)$$

$$0 \leq l_{t,\omega}^d \perp V^d + \lambda_{t,\omega} \geq 0 \quad (7f)$$

Least-cost mFRR activation ensures that the marginal cost of mFRR, the mFRR price in a mFRR activation auction, is equal to the expectation of the

mean of $\lambda_{t,\omega}$. This dual variable can be assimilated interpreted as a short-term price. It can also be equal to the marginal cost of aFRR activation under certain conditions. For every scenario and period, there are five possible cases.

1. There is no binding ramp constraint for aFRR. This means that all μ are equal to 0 and that $\lambda_{t,\omega}$ is equal to either the marginal cost of aFRR up or down. This assumes that the marginal loss incurred when deviating from balance is always greater than the marginal cost of aFRR. Note that it is impossible to get both upward and downward aFRR activation in this setting and that this case is equivalent to the problem presented in Eqs (1) and (2) of the main paper in which upward and downward inverse supply curves are aggregated and upward and downward activation are represented by the same variable.
2. aFRR up is constrained down (or at zero), and aFRR down is constrained up. This means that there is a positive imbalance that cannot be covered and that $l_{t,\omega}^d$ is greater than zero. This results in

$$\lambda_{t,\omega} = V^d. \quad (8)$$

3. aFRR up is constrained up, and aFRR down is constrained down (or at zero). This means that there is a negative imbalance that cannot be covered and that $l_{t,\omega}^u$ is greater than zero. This results in

$$\lambda_{t,\omega} = -V^u. \quad (9)$$

4. aFRR up is constrained up or down and aFRR down is not constrained. aFRR down is marginal so

$$\lambda_{t,\omega} = -O^{F,d}(x_{t,\omega}^{F,d}). \quad (10)$$

5. aFRR up is not constrained and aFRR down is constrained up or down. aFRR up is marginal and

$$\lambda_{t,\omega} = O^{F,u}(x_{t,\omega}^{F,u}). \quad (11)$$

Note that estimating the cost incurred when deviating from balance is not straightforward. Transient deviations can be sustained with little security risk but this impacts the *quality of the power*. TSOs are assessed based on the quality of their power and need to respect some European target.

Lemma 2 of the main paper is not influenced by the ramp constraints and the introduction of upward and downward balancing energy markets.

3 Empirical Data Analysis

This section presents the results of the experiment based on empirical data used to validate the equilibrium framework. The analysis investigates how the “less mFRR” activation strategy and different imbalance pricing schemes influence self-dispatch behavior, agent payoffs, and total activation costs.

3.1 Merit Order Approximation

The original merit-order curves that were sourced from real-world data for both fast and slow reserves were observed to be piecewise constant. While this reflects the nature of simple market orders, it introduces discontinuities that limit the applicability of the equilibrium formulation, which assumes continuous merit-order functions and smooth trade-offs between reserve types. To address this, the aggregated curves were approximated with piecewise linear functions.

3.2 Market Behavior and Self-Dispatch

At each point of discontinuity, a steep linear segment was added to bridge the price gap with a minimal volume change, while the flat parts of the simple blocks were represented with segments that have a low slope to maintain the general shape of the curve. In addition, the final segment of the fast merit-order curve (in both directions) was extended to reach a total capacity of 1000 MW, because the capacity limits of both fast and slow reserves are assumed to be sufficiently large to accommodate the maximum possible system imbalance across all scenarios. Figures 5 and 6 illustrate these transformations. Figure 5 shows the merit order of slow agents and its linear approximation, while Figure 6 shows the merit order of fast agents together with the extended curve that is used for the analysis.

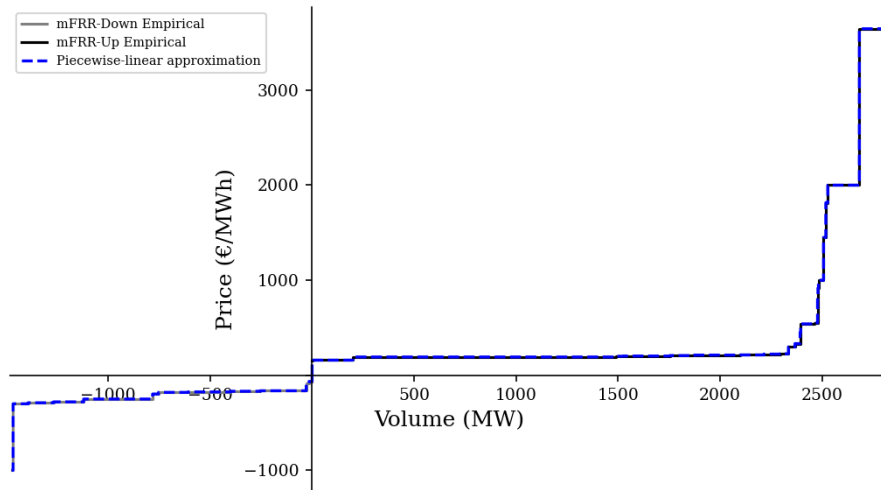


Figure 5: Aggregated merit order of slow agents: empirical data and piecewise linear approximation.

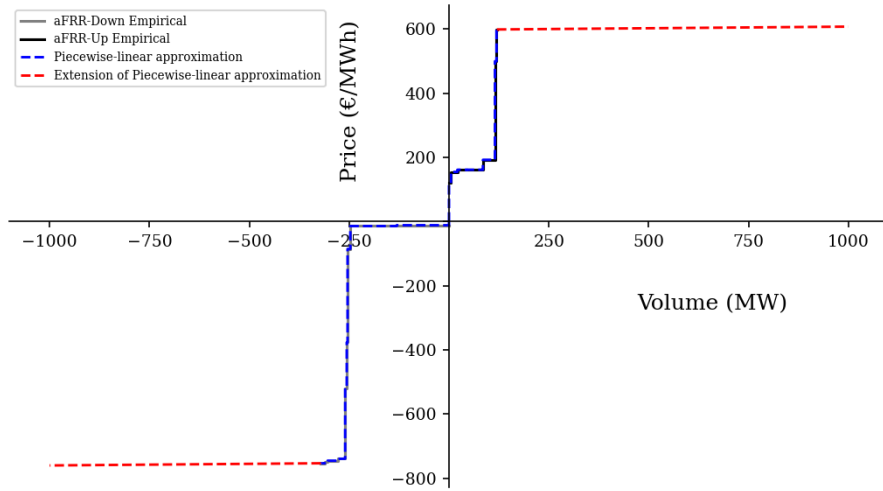


Figure 6: Aggregated merit order of fast agents: empirical data and piecewise linear approximation.

Using these approximated merit-order curves, the analysis first explored the least-cost mFRR activation strategy as a function of system imbalance forecast. Figure 7 presents the resulting optimal piecewise linear activation strategy, which serves as a baseline for comparing alternative activation strategies.

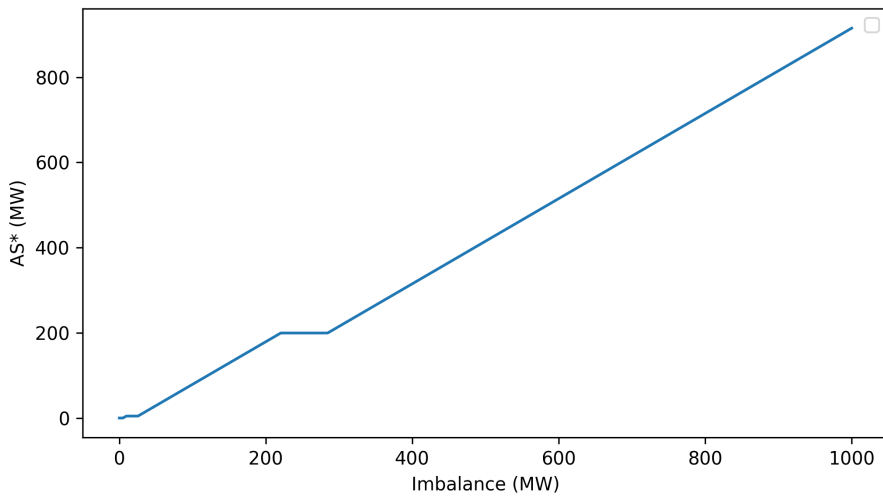


Figure 7: Least-cost mFRR activation strategy curve as a function of system imbalance forecast.

The analysis evaluates cases where the system operator activates less mFRR than the least-cost benchmark, representing a conservative reserve deployment strategy. Figure 8 presents the resulting level of self-dispatch for such a strategy under two pricing schemes: “mean mFRR and aFRR” and “max mFRR and mean aFRR”. In both cases, withheld capacity increases with the imbalance forecast, indicating that agents increasingly prefer to self-dispatch as potential payoffs grow.

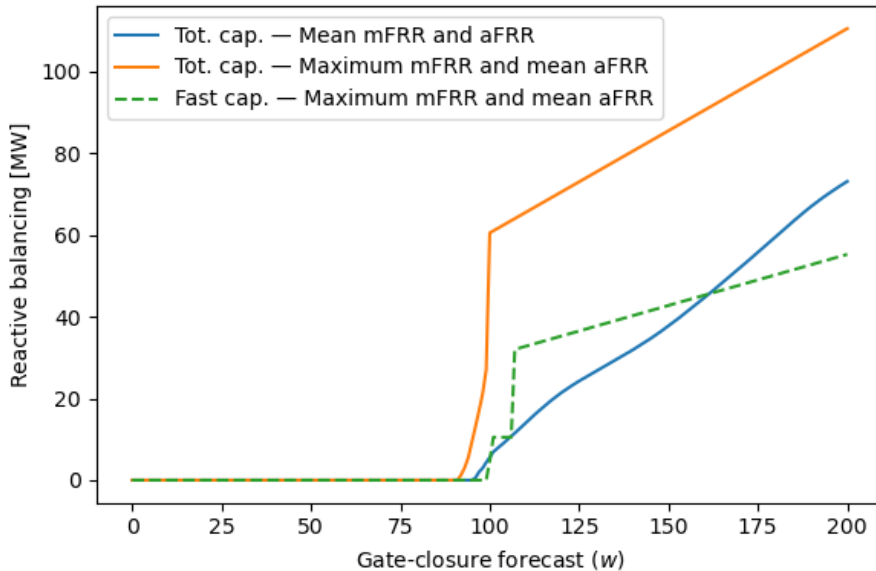


Figure 8: Comparison of fast and slow assets’ self-dispatching under the “less mFRR” activation strategy ($AS(y) = 0.5 \cdot AS^*(y)$) for the “mean mFRR and aFRR” and “max mFRR and mean aFRR” imbalance pricing schemes, when $X|y \sim U[y - 100, y + 100]$.

As shown in Figure 8, under the “max mFRR and mean aFRR” imbalance pricing scheme, the analysis revealed a distinct shift around 100 MW. Below this threshold, only slow agents self-dispatch, while above it, fast agents also begin to withhold capacity from the market. This change marks the point where the mFRR price overtakes the mean aFRR price and starts driving the overall imbalance price, altering the incentives for fast agents.

Another experiment evaluated how self-dispatch affects agents’ expected revenues. Figure 9 demonstrates that for a gate-closure forecast of 140 MW, self-dispatch consistently yields higher payoffs than participating in the mFRR auction under both “mean mFRR and aFRR” and “max mFRR and mean aFRR” imbalance pricing schemes. However, under the “mFRR” only imbalance pricing scheme, the agents appear nearly indifferent between self-dispatching and participating in the mFRR balancing energy auction.

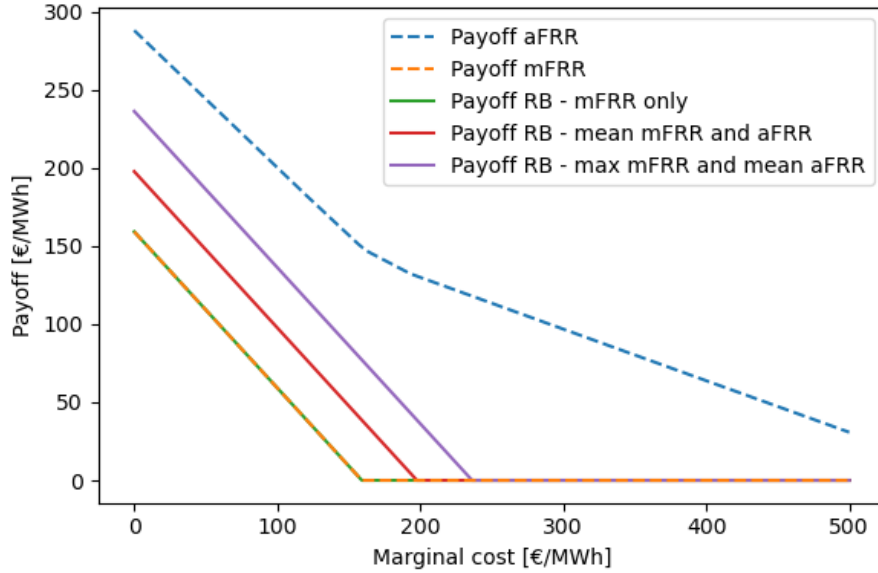
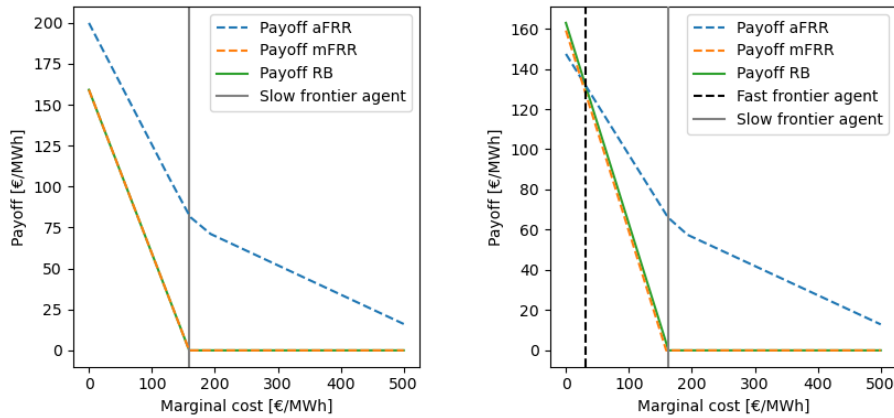


Figure 9: Effect of self-dispatching on expected agent payoffs as a function of marginal cost for a given gate-closure forecast $w = 140$ and $AS(y) = 0.5 \cdot AS^*(y)$, when $X|y \sim U[y - 100, y + 100]$.



(a) “mean mFRR and aFRR” imbalance pricing scheme.

(b) “max mFRR and mean aFRR” imbalance pricing scheme.

Figure 10: Effect of self-dispatching on expected agent payoffs as a function of marginal cost for a gate-closure forecast $w = 140$ and activation strategy $AS(y) = 0.5 \cdot AS^*(y)$, when $X|y \sim U[y - 100, y + 100]$.

Figure 10a focuses on the “mean mFRR and aFRR” imbalance pricing scheme. Here, self-dispatching by slow agents lowers the residual imbalance that is left for fast reserves, which in turn pushes aFRR prices down. Interestingly, the mFRR price remains almost unchanged due to the flat segments in the merit-order curve, meaning that removing some cheap self-dispatching capacity does not shift the clearing price significantly.

Under the “max mFRR and mean aFRR” imbalance pricing scheme, shown in Figure 10b, the pattern is similar but more pronounced. Self-dispatch continues to dominate auction participation in terms of payoffs, yet the mFRR price remains relatively stable while the aFRR price decreases due to the reduced residual imbalance.

3.3 System Activation Costs

Figure 11 summarizes the impact on total system costs across the different activation strategies and imbalance pricing schemes. The results show that the “max mFRR and mean aFRR” imbalance pricing scheme leads to the highest overall costs in all scenarios that were examined. The comparison between “mean mFRR and aFRR” and “mFRR only” depends on both the level of activation and the accuracy of forecasts, suggesting that no single imbalance pricing scheme dominates under all conditions.

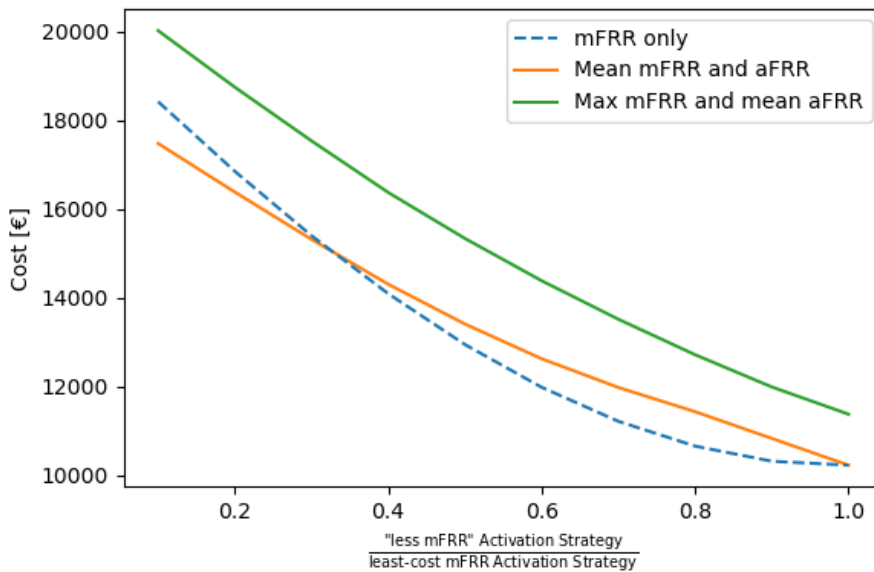


Figure 11: Comparison of activation costs across the examined imbalance pricing schemes as a function of activation strategy to least-cost mFRR activation strategy ratio, when $X|y \sim U[y - 100, y + 100]$.

3.4 Key Insights

The experiment provides several results that complement the main analysis:

1. The equilibrium structures identified in the theoretical model are robust to the use of approximated empirical merit-order curves.
2. Conservative activation strategies and less accurate forecasts both encourage agents to self-dispatch earlier, at lower gate-closure imbalance levels.
3. The “max mFRR and mean aFRR” imbalance pricing scheme consistently produces the highest activation costs and amplifies the effects of suboptimal activation strategies.
4. System operator forecast accuracy plays a central role in determining both total system costs and the profitability of self-dispatching.

Overall, the experiment based on empirical data confirms that the patterns identified in the main paper persist when tested against realistic merit-order curves.